Supplementary Information (SI) for Journal of Materials Chemistry A.

Supporting Information

Graphene Acid-enhanced Interfacial Layers with High Zn^{2+} Ions Selectivity and Desolvation Capability for Corrosion-resistant Zn-metal Anodes

Kailai Xia,[a] Liuyan Li,[a] Yanbin Qiu,[a] Jianqiang Weng,[a] Shengtao Shen,[a] Meixin,[a] Yuhang Zhuang,[a] Yeye Wen,*[b] Chengkai Yang,*[a] Zheyuan Liu,[a] Mingmao Wu,*[a,c] Zhigang Zou[d]

[a] Key Laboratory of Advanced Materials Technologies, International (HongKong Macao and Taiwan) Joint Laboratory on Advanced Materials Technologies, College of Materials Science and Engineering, Fuzhou University, Fuzhou, 350108, P. R. China

[b] Advanced Research Institute of Multidisciplinary Science, Beijing Institute of Technology, Beijing, 100081, P. R. China

[c] Fujian Science & Technology Innovation Laboratory for Optoelectronic Information of China, Fuzhou, Fujian 350108, P. R. China

[d] National Laboratory of Solid State Microstructures, Department of Physics, Nanjing University, Nanjing, 210093, P. R. China

*Corresponding authors.
E-mail:wumm20@fzu.edu.cn (M. M. Wu); chengkai_yang@fzu.edu.cn (C. K. Yang); wenyy@bit.edu.cn (Y. Y. Wen).

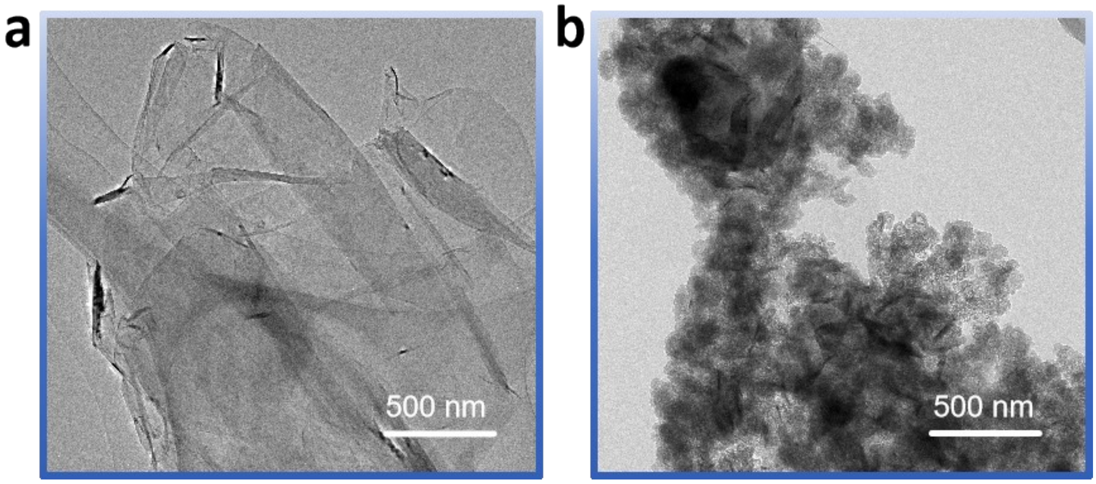

Fig. S1. TEM images of (a) GO and (b) GA.

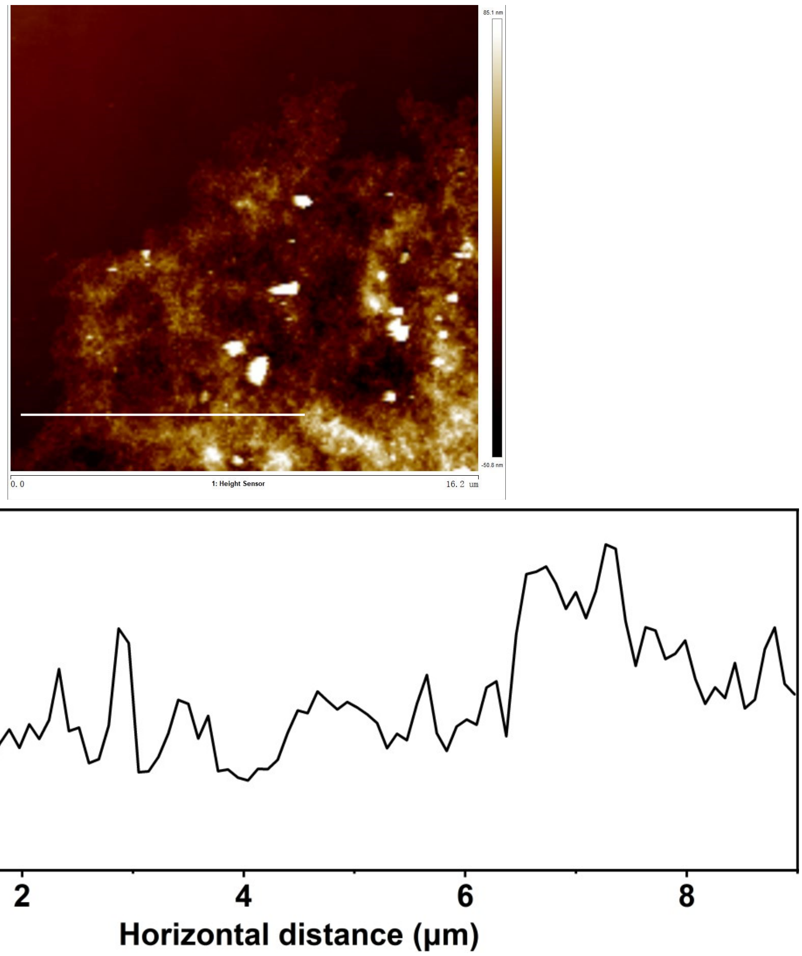

Fig. S2. AFM morphology of GA and corresponding height profiles.

Fig. S3. Digital images of CNF membrane and CNF/GA membrane measured with vernier calipers.

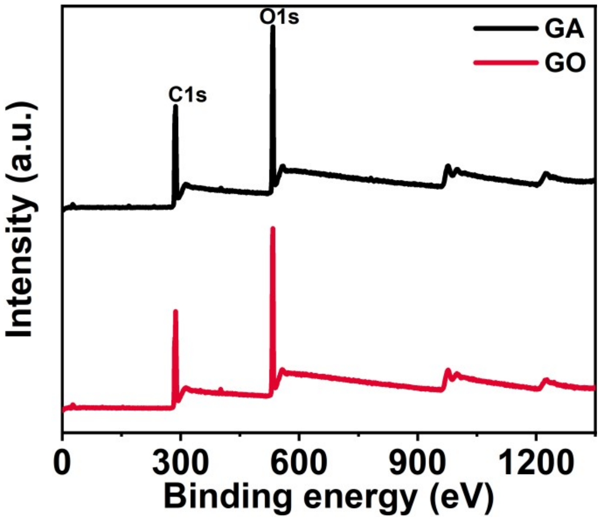

Fig. S4. XPS spectra of GO and GA.

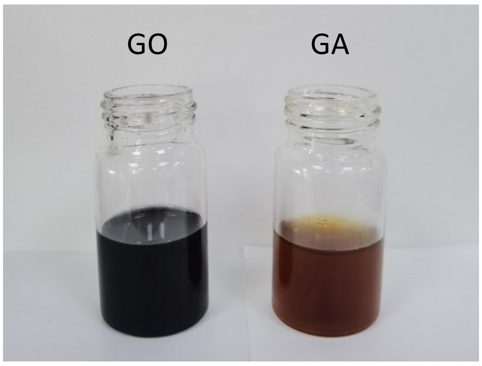

Fig. S5. Digital image of 5 mg mL^{-1} GO and GA solutions.

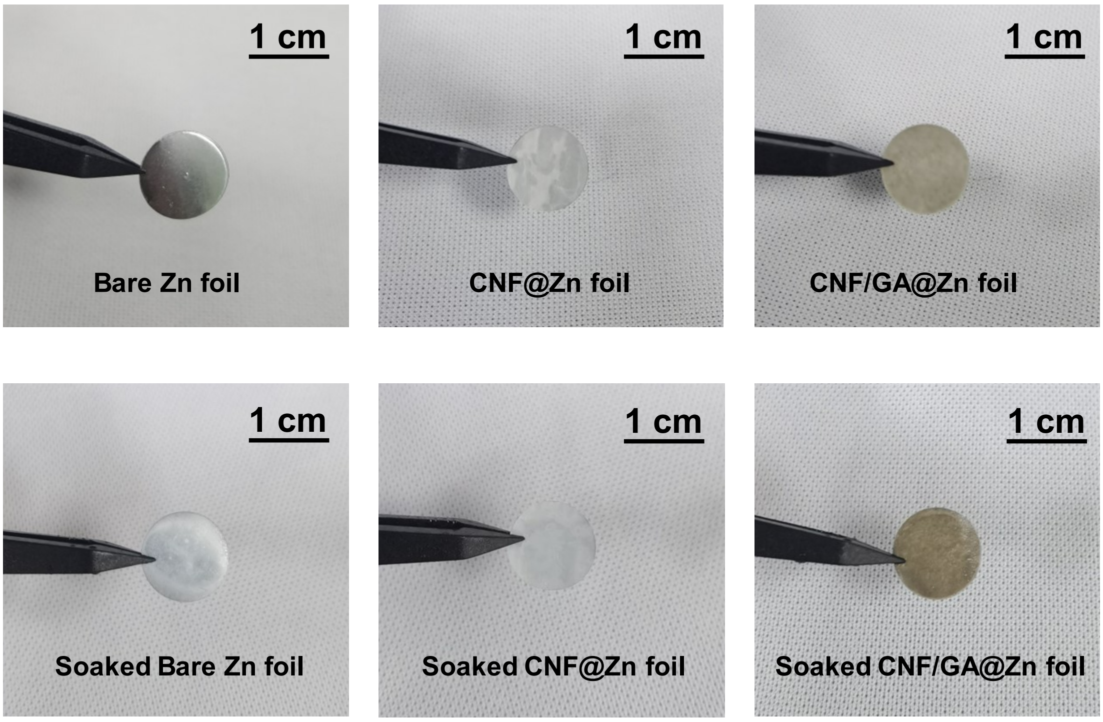

Fig. S6. Digital images of the bare Zn, CNF@Zn, and CNF/GA@Zn anodes before (upper row) and after soaking (lower row) in 2 M $ZnSO_4$ electrolyte for 7 days.

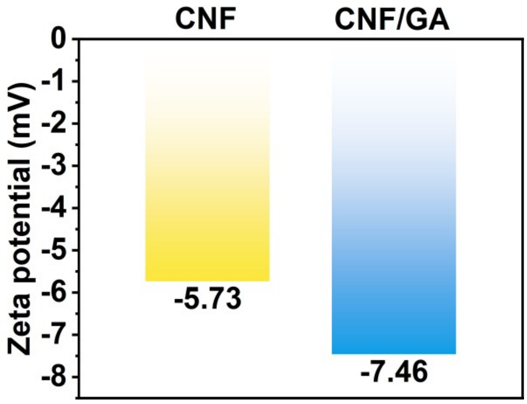

Fig. S7. The Zeta potential of CNF and CNF/GA solutions.

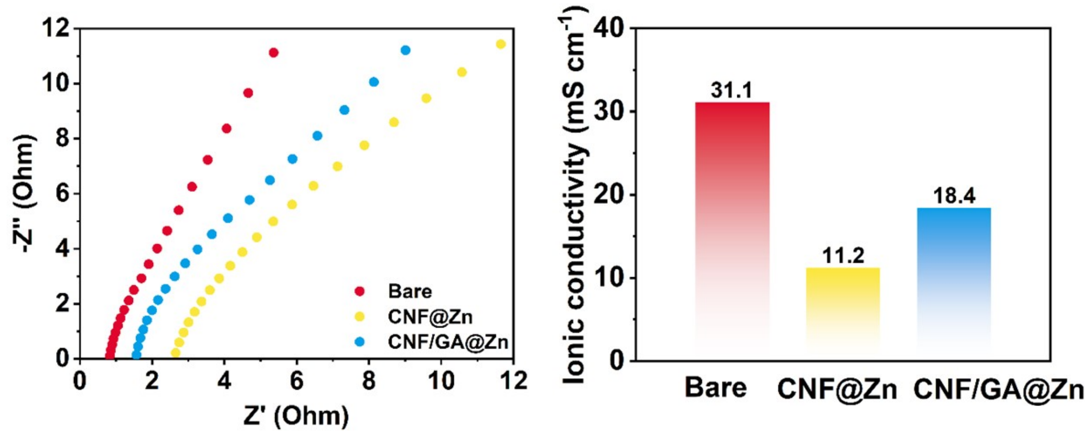

Fig. S8. Ionic conductivity of the symmetric cells based on bare Zn, CNF@Zn, and CNF/GA@Zn anodes.

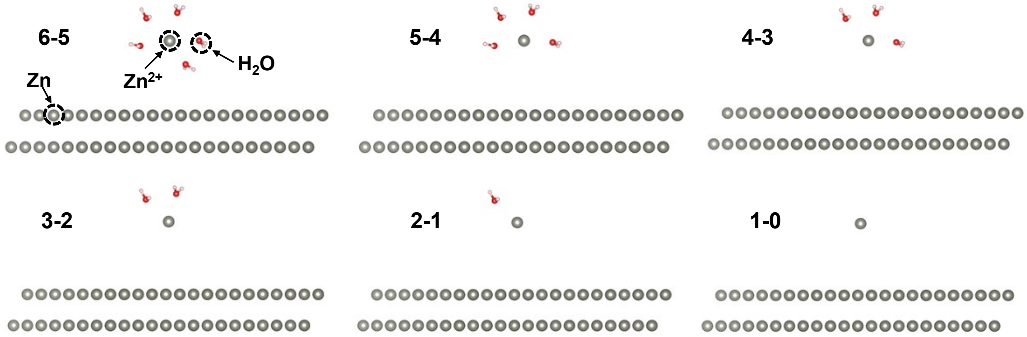

Fig. S9. Simulated desolvation process of Zn^{2+} ions by sequential removal of 6 H_2O on bare Zn surface.

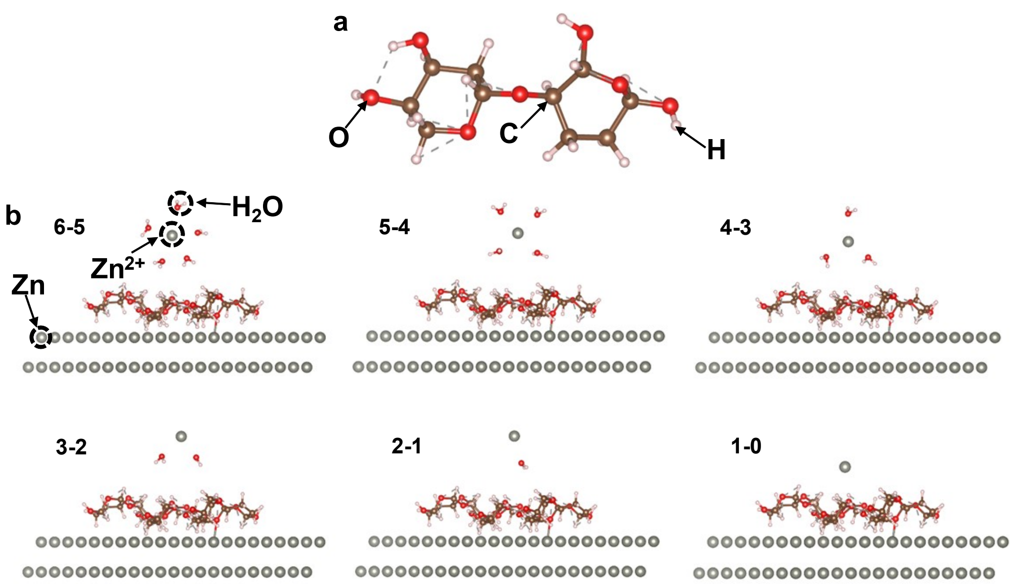

Fig. S10. (a) Constructed CNF molecular structure model. (b) Simulated desolvation process of Zn^{2+} ions by sequential removal of six H_2O on CNF@Zn surface.

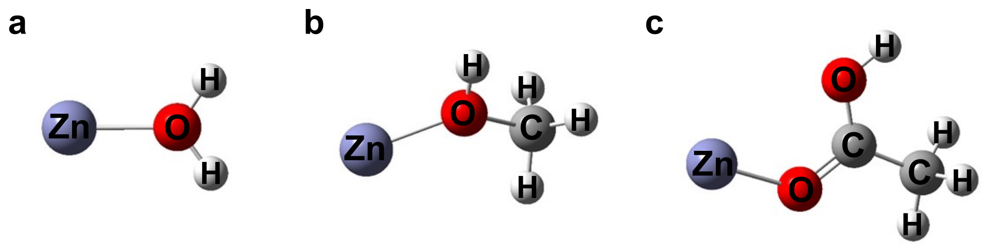

Fig. S11. Simulated binding energy between Zn^{2+} ions and (a) H_2O, (b) -OH, (c) -COOH.

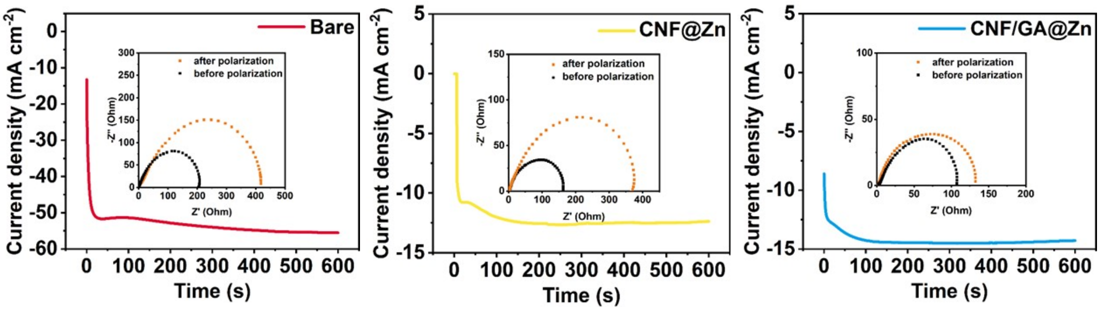

Fig. S12. Current-time plots of the symmetric cells based on bare Zn, CNF@Zn, and CNF/GA@Zn anodes (inset: the Nyquist polts before and after polarization).

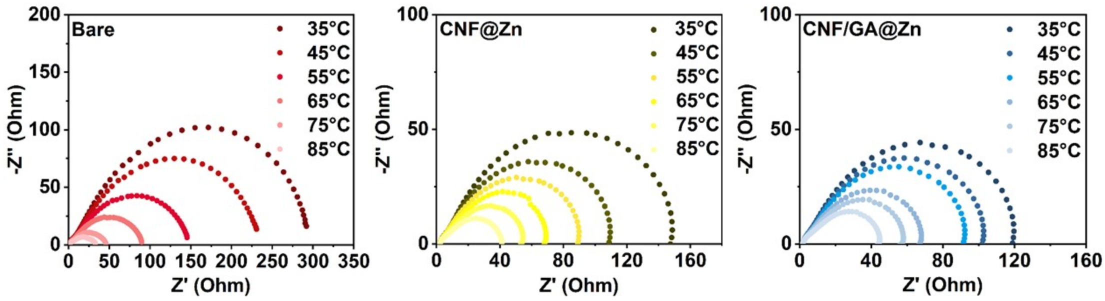

Fig. S13. Nyquist plots of the symmetric cells based on bare Zn, CNF@Zn, and CNF/GA@Zn anodes at the temperature of 35 °C, 45 °C, 55 °C, 65 °C, 75 ℃, and 85 °C.

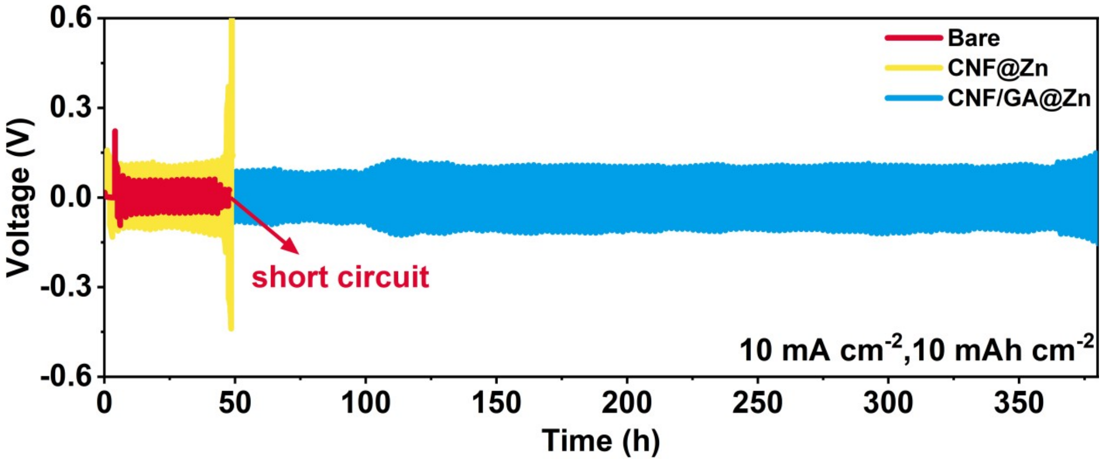

Fig. S14. Long-term cycling performance of the symmetric cells based on bare Zn, CNF@Zn, and CNF/GA@Zn anodes at a current density of 10 mA cm^{-2} with a capacity of 10 mAh cm^{-2}.

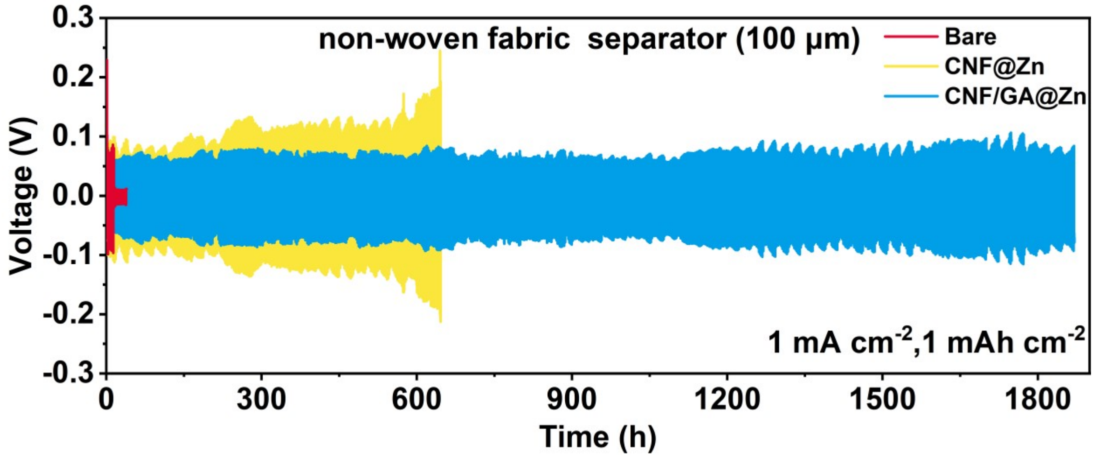

Fig. S15. Long-term cycling performance of symmetric cells assembled with non-woven seperators at 1 mA cm^{-2} and 1 mAh cm^{-2}.

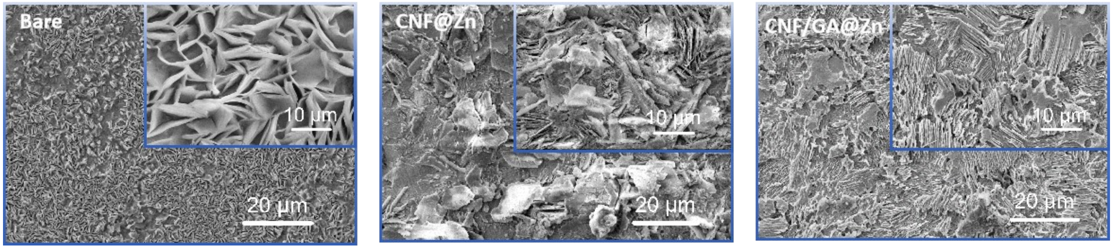

Fig. S16. SEM images of bare Zn, CNF@Zn, and CNF/GA@Zn after 1 cycle at the current density of 1 mA cm^{-2} with a capacity of 1 mAh cm^{-2}

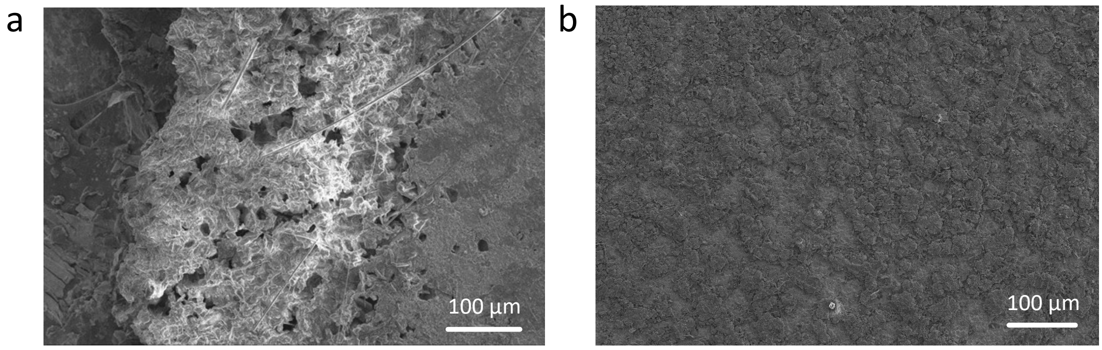

Fig. S17. SEM images of (a) bare Zn and (b) CNF/GA@Zn surface after cycling at 1 mA cm^{-2}, 1 mAh cm^{-2} for 300 hours.

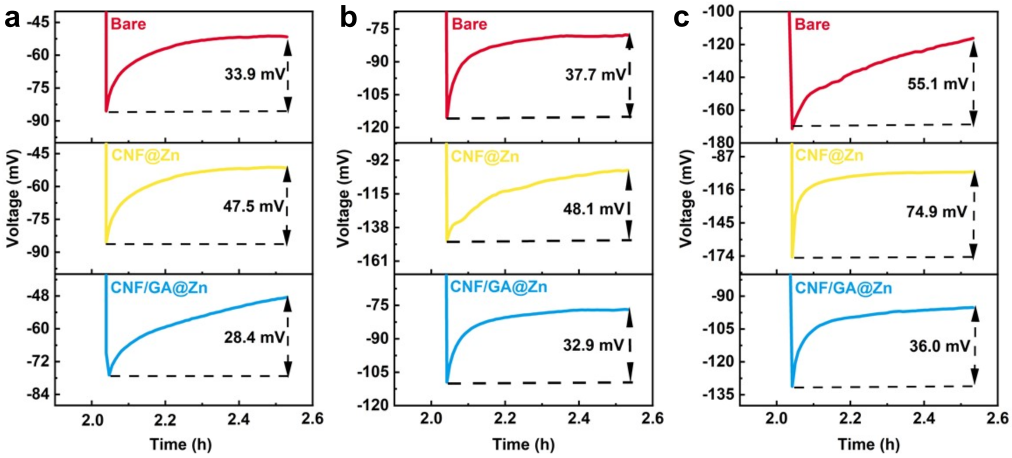

Fig. S18. Nucleation overpotential of the symmetric cells based on bare Zn, CNF@Zn, and CNF/GA@Zn at different densities of (a) 1 mA cm^{-2}, 1 mAh cm^{-2}, (b) 5 mA cm^{-2}, 5 mAh cm^{-2} and (c) 10 mA cm^{-2}, 10 mAh cm^{-2}.

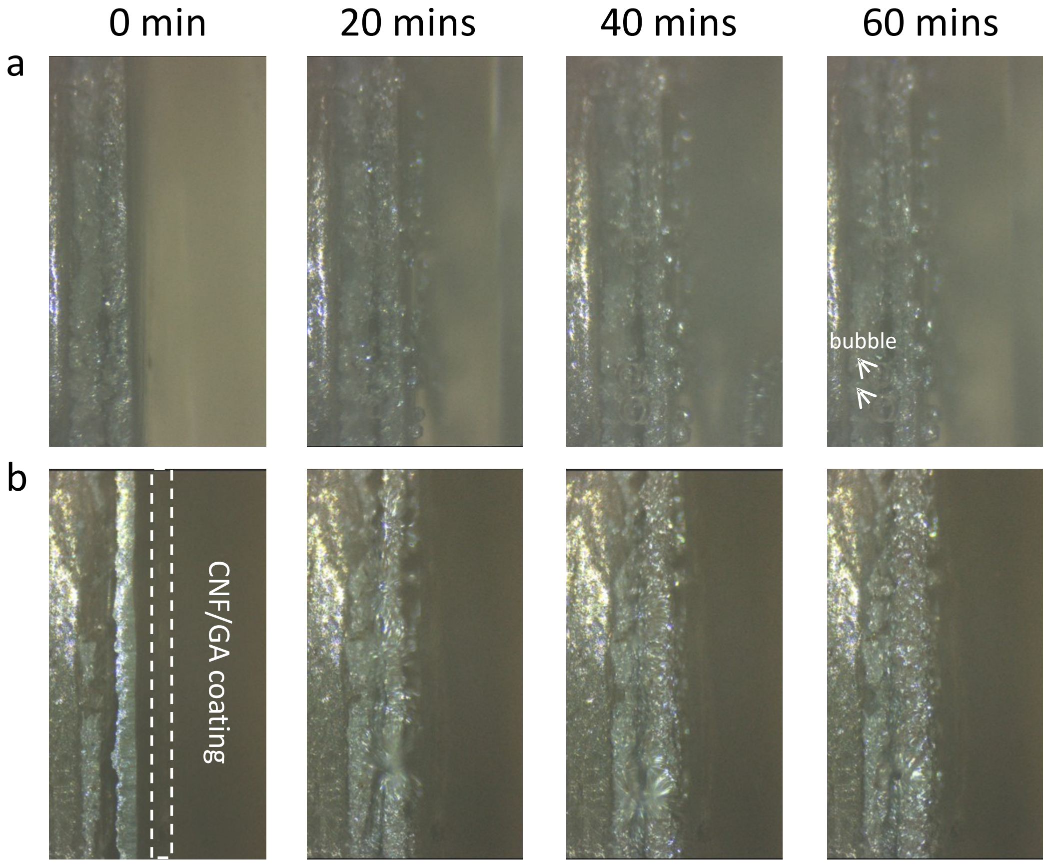

Fig. S19. Situ optical microscopy image of (a) bare Zn and (b) CNF/GA@Zn surface after depositing at 10 mA cm^{-2} for 0, 20, 40, 60 mins.

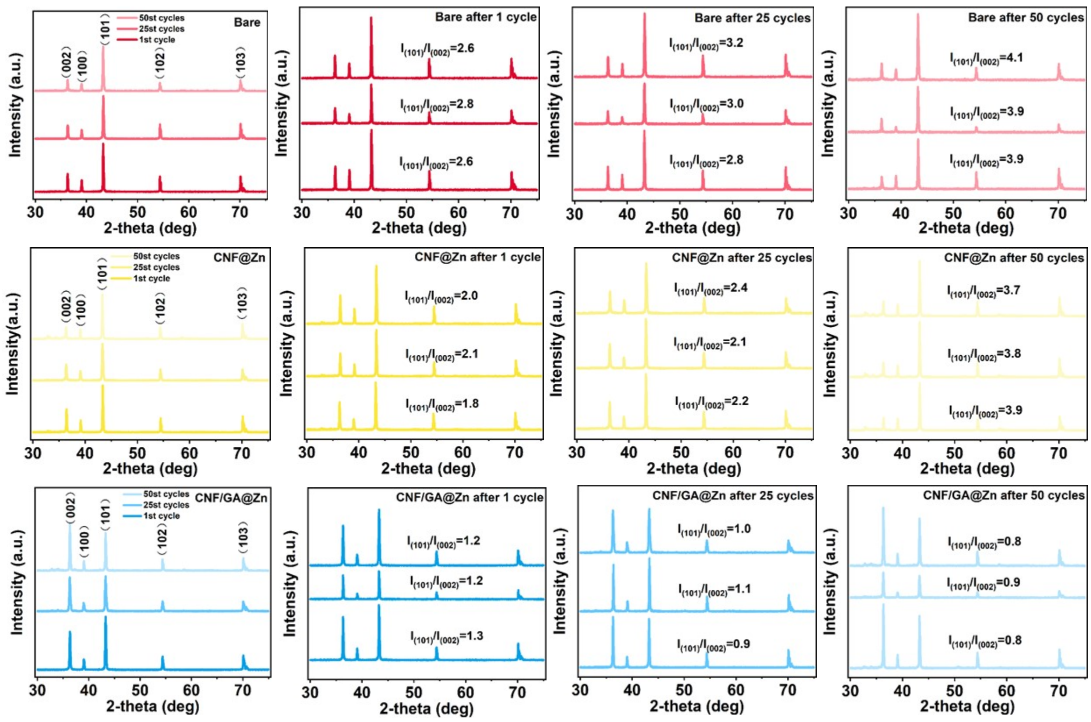

Fig. S20. XRD patterns at three different positions on the surface of the Zn anode after 1, 25, and 50 cycles at 1 mA cm^{-2}, 1 mAh cm^{-2}.

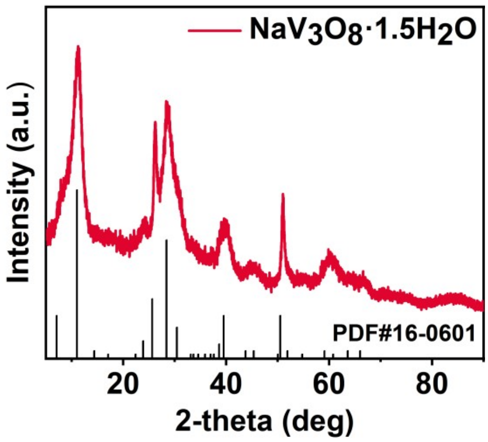

Fig. S21. XRD curve of the $NaV_3O_8·1.5H_2O$.

Table S1. Comparison of electrochemical performance of the different Zn anode protection scheme for symmetric cells

Anode	Current density and capacity	Cycle life	Reference
NGO[a)]	1 mA cm^{-2}, 1 mAh cm^{-2}	1200 h	[S1]
CNF/Zn@Zn[b)]	2 mA cm^{-2}, 1 mAh cm^{-2}	260 h	[S2]
NBC@Zn[c)]	2 mA cm^{-2}, 1 mAh cm^{-2}	1200 h	[S3]
CAZ@Zn[d)]	1 mA cm^{-2}, 1 mAh cm^{-2}	2750 h	[S4]
Sep-OH[e)]	5 mA cm^{-2}, 1 mAh cm^{-2}	800 h	[S5]
CNF-SO_3Zn[f)]	1 mA cm^{-2}, 0.5 mAh cm^{-2}	100 h	[S6]
CNF/MXene@Zn[g)]	1 mA cm^{-2}, 1 mAh cm^{-2}	2800 h	[S7]
SA-coated Zn[h)]	0.5 mA cm^{-2}, 0.5 mAh cm^{-2}	920 h	[S8]
ZC separator[i)]	0.5 mA cm^{-2}, 0.25 mAh cm^{-2}	2000 h	[S9]
	1 mA cm^{-2}, 1 mAh cm^{-2}	2920 h	
CNF/GA@Zn	5 mA cm^{-2}, 5 mAh cm^{-2}	850 h	This work
	10 mA cm^{-2}, 10 mAh cm^{-2}	380 h	

[a)] NGO = an artificial interface film of nitrogen (N)-doped graphene oxide;
[b)] CNF/Zn@Zn = a lightweight and flexible three-dimensional carbon nanofiber architecture with uniform Zn seeds prepared from bacterial cellulose;
[c)] NBC@Zn = an amino-grafted bacterial cellulose film;
[d)] CAZ@Zn = an ion-affiliative cellulose acetate coating with $Zn(CF_3SO_3)_2$;
[e)] Sep-OH = a coating prepared from sepiolite and its derived materials;
[f)] CNF-SO_3Zn = a multifunctional aqueous ZB separator based on a single-ion-functionalized cellulose nanofiber membrane;
[g)] CNF/MXene@Zn = a cellulose nanofiber/MXene composite membrane;
[h)] SA-coated Zn = an anionic polyelectrolyte alginate acid coating;
[i)] ZC separator = a cellulose nanofibers-ZrO_2 composite separator;

Table S2. Comparison of Self-discharge performance of the different Zn anode protection scheme for full cells

Programme	Cathode	standing time	Capacity retention	Reference
CS and SA coating[a)]	$H_2V_3O_8$	24 h	85%	[S10]
Na_3NTA additive[b)]	V_2O_5	24 h	83%	[S11]
KTPP additive[c)]	MnO_2	24 h	88%	[S12]
NBC layer	V_2O_5	24 h	94.94%	[S3]
β-CD additive[d)]	V_2O_5	36 h	71%	[S13]
ACE additive[e)]	V_2O_5	24 h	82.95%	[S14]
Irgacure 2959 additive[f)]	VS_2	24 h	96.4%	[S15]
Thiourea additive	V_2O_5	24 h	98.03%	[S16]
CNF/GA coating	NVO	24 h	99%	This work

[a)] CS and SA coating = a film consisted by chitosan and sodium alginate;

[b)] Na_3NTA additive = trisodium nitrilotriacetate;

[c)] KTPP additive = penta-potassium triphosphate electrolyte;

[d)] β-CD additive = β-cyclodextrin electrolyte;

[e)] ACE additive = acesulfame electrolyte;

[f)] Irgacure 2959 additive = 2-Hydroxy-4′-(2-hydroxyethoxy)-2-methylpropiophenon;

References
[S1]L. Kang, J. Zheng, K. Yue, H. Yuan, J. Luo, Y. Wang, Y. Liu, J. Nai and X. Tao, Small, 2023, 19, 2304094.
[S2]X. Liu, Q. Han, Q. Ma, Y. Wang and C. Liu, Small, 2022, 18, 2203327.
[S3]X. Ge, W. Zhang, F. Song, B. Xie, J. Li, J. Wang, X. Wang, J. Zhao and G. Cui, Adv. Funct. Mater., 2022, 32, 2200429.
[S4]H. Dong, X. Hu, R. Liu, M. Ouyang, H. He, T. Wang, X. Gao, Y. Dai, W. Zhang, Y. Liu, Y. Zhou, D. J. L. Brett, I. P. Parkin, P. R. Shearing and G. He, Angew. Chem., Int. Ed., 2023, 62, e202311268.
[S5]W. Xu, X. Liao, W. Xu, K. Zhao, G. Yao and Q. Wu, Adv. Energy Mater., 2023, 13, 2300283.
[S6]J. Cao, D. Zhang, C. Gu, X. Zhang, M. Okhawilai, S. Wang, J. Han, J. Qin and Y. Huang, Nano Energy, 2021, 89, 106322.
[S7]Y. Wang, X. Lin, L. Wang, Y. Yang, Y. Zhang and A. Pan, Adv. Funct. Mater., 2023, 33, 2211088.
[S8]J.-H. Wang, L.-F. Chen, W.-X. Dong, K. Zhang, Y.-F. Qu, J.-W. Qian and S.-H. Yu, ACS Nano, 2023, 17, 19087–19097.
[S9]J. Zhou, M. Xie, F. Wu, Y. Mei, Y. Hao, R. Huang, G. Wei, A. Liu, L. Li and R. Chen, Adv. Mater., 2021, 33, 2101649.
[S10] X. Cai, X. Wang, Z. Bie, Z. Jiao, Y. Li, W. Yan, H. J. Fan and W. Song, Adv. Mater., 2024, 36, 2306734.
[S11] H. Qin, W. Kuang, N. Hu, X. Zhong, D. Huang, F. Shen, Z. Wei, Y. Huang, J. Xu and H. He, Adv. Funct. Mater., 2022, 32, 2206695.
[S12] Q. Guan, J. Li, L. Li, P. Chai, Y. Li, S. Zhang, X. Yu, L. Bao, J. Peng and X. Li, Chem. Eng. J., 2023, 476, 146534.
[S13] T. C. Li, C. Lin, M. Luo, P. Wang, D.-S. Li, S. Li, J. Zhou and H. Y. Yang, ACS Energy Lett., 2023, 8, 3258–3268.
[S14] Z. Jiao, X. Cai, X. Wang, Y. Li, Z. Bie and W. Song, Adv. Energy Mater., 2023, 13, 2302676.
[S15] Y. Yu, P. Zhang, W. Wang and J. Liu, Small Methods, 2023, 7, 2300546.
[S16] C. Meng, W. He, L. Jiang, Y. Huang, J. Zhang, H. Liu and J.-J. Wang, Adv. Funct. Mater., 2022, 32, 2207732.